Pergamon

Pattern Recognition, Vol. 29, No. 6, pp. 997–1005, 1996
Elsevier Science Ltd
Copyright © 1996 Pattern Recognition Society
Printed in Great Britain.
0031-3203/94 $15.00 + 00

0031-3203(96)00130-1

A SIMPLIFIED FOLD NUMBER DETECTOR FOR SHAPES WITH MONOTONIC RADII

JA-CHEN LIN
Department of Computer and Information Science, National Chiao Tung University, Hsinchu, Taiwan, R. O. C.

(*Received* 17 *March* 1995; *in revised form* 7 *August* 1995; *received for publication* 29 *August* 1995)

Abstract—This paper concentrates on the fold number detection problem for the shapes with monotonic radii. The proposed method is extremely simple. Two monotonicity conditions are derived to ensure that the smallest positive integer l making $\iint_{(r,\theta)\in S} r^2 e^{il\theta} dr\, d\theta$ nonzero is exactly the fold number of the given shape S. The fold numbers of regular polygons, roses, bolt nuts, and other kinds of shapes discussed in the present paper, can therefore be detected quite easily. Note especially that the proposed method uses no matching procedure, a procedure essential in many reported methods. Theoretical properties, mathematical proofs, illustrative figures, and experimental results, are all included in this paper. Copyright © 1996 Pattern Recognition Society. Published by Elsevier Science Ltd.

Rotational symmetry Mirror symmetry Monotonicity Rotation-matching
Regular polygons Bolt nuts Roses

1. INTRODUCTION

An important shape feature, which is widely used in shape recovery,[1] shape registration,[2,3] shape storage space reduction,[4] etc., is the so-called symmetry property. At least two kinds of symmetry can be identified, namely, mirror symmetry[5,6] and rotation symmetry.[7] To make use of the shape symmetry property, it is necessary to compute either the number of symmetry axes or the number of folds of a given shape. Several methods[5,6,8] have been proposed to find the number of the symmetry axes of a given mirror symmetric shape (i.e., symmetric about certain lines called symmetry axes). On the other hand, the number of folds n of a given rotationally symmetric shape can be detected by the methods described in References (1), (2) and (5). Highnam[5] used a string matching technique to detect n, whereas Leou and Tsai[2] counted as n the frequency that the boundary of the given rotationally symmetric shape runs across a special circle related to the given shape. Recently, Lin *et al.* proposed a simpler method in Reference (1) to detect n based on a simple mathematical property of rotationally symmetric shapes. Note that these methods require the use of certain matching techniques: string matching is used in Reference (5), whereas shape matching is used in both References (1) and (2). Lin *et al.* had pointed out in Reference (1) that their method has an extra benefit that once the fold number is obtained, the shape orientation can also be obtained immediately by a time-negligible step: a simple call of the arc-tangent function followed by an arithmetic division. We therefore concentrate the study on the method of Lin *et al.*, and try to discover some more mathematical properties of the method. More precisely, we will investigate what will happen if the method is applied to a special branch of the rotationally symmetric shapes, namely, the rotationally symmetric shapes of which the polar radii are monotonic in a fold (or in a half-fold if the fold itself is also mirror-symmetric). This special branch includes regular polygons, bolt nuts, roses and so on. It will be proved that many procedures used by Lin *et al.*, including the matching procedure, can be discarded. As a result, if the image processing environment (also called the processing domain) is limited to the collection of all regular polygons, bolt nuts, roses and so on, then their method, which is already very attractive due to its certain properties [see the final section of Reference (1)], can be simplified further.

The remainder of the paper is organized as follows: in Section 2, the definitions of rotationally symmetric shapes and polar radii function are introduced, and the rotation matching procedure of Lin *et al.* is reviewed. The theory needed to simplify the method of Lin *et al.* is introduced in Sections 3 and 4. Experimental results are provided in Section 5, and a summary and some concluding discussion are given in Section 6. Most of the proofs are collected in an appendix to make the paper easier to read.

2. DEFINITIONS AND LIN *et al.*'s ROTATION-MATCHING TEST

A shape S is called an n-fold rotationally symmetric shape (abbreviated as an n-RSS henceforth) if it is identical to itself after being rotated around its centroid through any multiple of the angle $2\pi/n$ for some $n > 1$. For simplicity, assume that no other larger

integer n has this property. The goal of fold number detection is to find this value n when the given shape S has been known to be a rotationally symmetric shape. For convenience, the origin of the coordinate system is taken to be the centroid of S. Lin *et al.* used trigonometric identities to prove in Reference (1) a simple mathematical property. They then used this property to design a method for obtaining a value l_1, of which n is a factor. The exact value of n was then detected by a rotation-matching test. When the given rotationally symmetric shape meets certain monotonic conditions, however, it will be shown in the present paper that the rotation-matching test is not necessary. The value of n can therefore be detected in a much simpler way. The following two definitions will be used later to derive the monotonic condition just mentioned.

Definition 1.
In the polar coordinate system, the polar radii function $r_{\max}(\theta)$ of a shape S is defined by

$$r_{\max}(\theta) = \max_{(r,\theta)\in S} r \tag{1}$$

for each θ.
Note that every $(r_{\max}(\theta), \theta)$ is a point on the boundary of S.

Definition 2.
A shape S is said to be radially full if for every θ, the shape S can contain the whole line segment whose two ends are the centroid (i.e., the pole O) and the boundary point $(r_{\max}(\theta), \theta)$.

All shapes sketched in Fig. 2–5, except Fig. 4(e), are radially full whereas the shapes sketched in Fig. 1 and 6 are not. The shape in Fig. 1(a) is not considered radially full because the (dashed) line segment connecting A and the centroid O is not contained in the shape. Note that every (closed) convex set must be radially full (just use the fact that the centroid O of a convex set must be a point of the set,[9] and hence, the line segment connecting O and the point $[r_{\max}(\theta), \theta)$ must be in the set]; however, a radially full set need not be convex (for example, the shapes in Fig. 2 are radially full, although they are not convex).

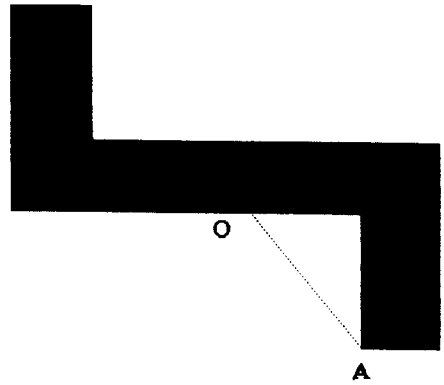

Fig. 1. A shape which is not radially full.

For a given (centralized) shape S, and for any natural number l, let $x^{(l)} + iy^{(l)}$ be defined by

$$x^{(l)} + iy^{(l)} = \int\int_{(x,y)\in S} |x+iy| \left(\frac{x+iy}{|x+iy|}\right)^l \mathrm{d}x\mathrm{d}y \tag{2}$$

$$= \int\int_{(x,y)\in S} re^{il\theta} \mathrm{d}x\mathrm{d}y \tag{3}$$

$$= \int\int_{(r,\theta)\in S} r^2 e^{il\theta} \mathrm{d}r\mathrm{d}\theta \tag{4}$$

where r and θ are defined by the convention $re^{i\theta} = x + iy$. In other words, θ is the polar angle of the point (x, y), and $r = |x+iy| = \sqrt{x^2+y^2}$ is the polar radius. Since the shape has been centralized, that is, since the coordinate system has been translated so that $\iint_{(x,y)\in S} x\,\mathrm{d}x\mathrm{d}y = \iint_{(x,y)\in S} y\,\mathrm{d}x\mathrm{d}y = 0$, the value of $x^{(l)} + iy^{(l)}$ is always zero if $l = 1$. When $l = 1, 2, 3, 4, \cdots$, the values of $x^{(l)} + iy^{(l)}$ are governed by Theorem 1, as given below. (The shape S needs not be radially full in this theorem.)

Theorem 1.
Let S be an n-RSS. If l/n is not an integer, then $x^{(l)} + iy^{(l)} = 0$.

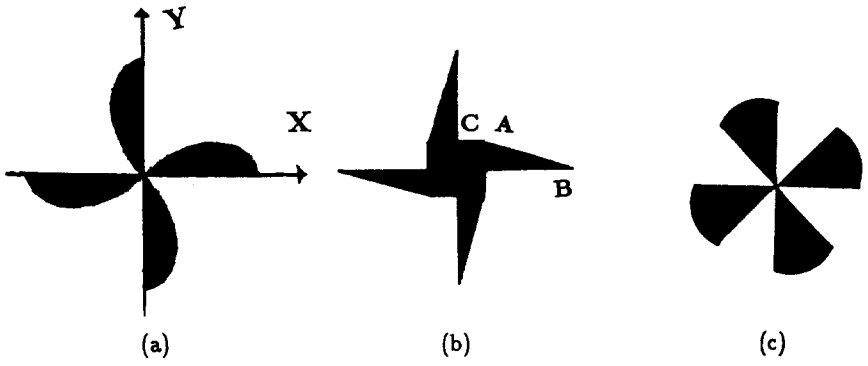

Fig. 2. Three shapes meeting the requirements listed in Theorem 2 and so satisfying $l_1 = n$.

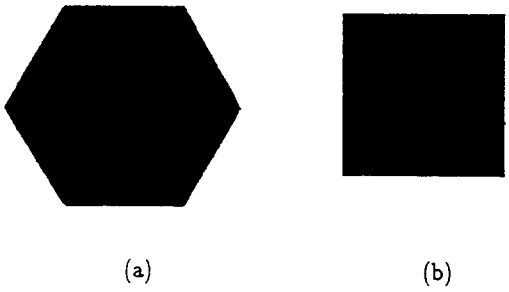

Fig. 3. Examples of regular polygons; (a) A polygon of 6 sides; (b) A polygon of 4 sides.

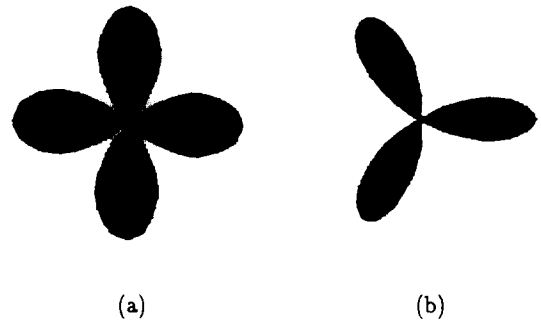

Fig. 5. Examples of Roses; (a) A 4-leafed rose; (b) A 3-leafed rose.

To prove this, we may decompose the integration in equation (4) as

$$\int_0^{2\pi} = \int_0^{2\pi/n} + \int_{2\pi/n}^{4\pi/n} + \int_{4\pi/n}^{6\pi/n} + \cdots + \int_{2(n-1)\pi/n}^{2\pi} \tag{5}$$

The fact that $(r, \theta) \in S$, if and only if $(r, \theta + 2\pi/n) \in S$, can then be used to derive $\int_{2\pi/n}^{4\pi/n} = e^{il2\pi/n} \int_0^{2\pi/n}$, $\int_{4\pi/n}^{6\pi/n} = e^{il4\pi/n} \int_0^{2\pi/n}$, etc. Equation (5) therefore becomes

$$\iint_{\{(r,\theta)\in S \mid 0 \le \theta < 2\pi/n\}} r^2 e^{il\theta}[1 + e^{il2\pi/n} + e^{il4\pi/n} + \cdots + e^{il(2n-2)\pi/n}]\,dr\,d\theta. \tag{6}$$

The integrand is zero because the sum in the bracket is the sum (which is zero) of the n roots of the equation $z^n - 1 = 0$.

Notice that Theorem 1 does not imply that $x^{(n)} + iy^{(n)} \neq 0$ although $n/n = 1$ is an integer. In fact, the author had inspected several examples and found that $x^{(n)} + iy^{(n)} \neq 0$ for some n-RSS, and that, $x^{(n)} + iy^{(n)} = 0$ for some other n-RSS. It is therefore not true to say that l_1, which is defined to be the smallest positive value l making $x^{(l)} + iy^{(l)}$ non-zero, is the value n we want. However, using the fact that n must be a factor of l_1, together with the definition of n-RSS, people may employ a rotation-matching test, as used by Lin *et al.*, to determine the value of n. The detail is as follows: evaluate $x^{(l)} + iy^{(l)}$ for $l = 2$, then, for $l = 3$, and so on, until $x^{(l)} + iy^{(l)} \neq 0$ occurs. Let the value of l used in that iteration be $l = l_1$. Then, as stated above, it is not true to say that l_1 is the value n we want. However, Theorem 1 implies that n must be a factor of this l_1. (Otherwise, l_1/n is not an integer, and hence, $x^{(l_1)} + iy^{(l_1)} = 0$, which contradicts the definition of l_1).

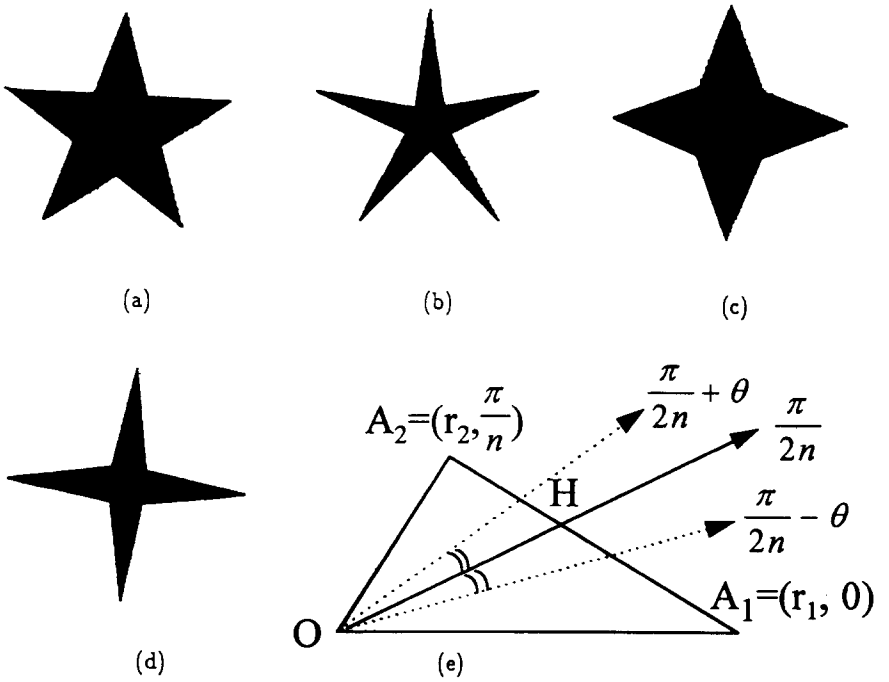

Fig. 4. Examples of regular stars; (a) and (b) two 5-leafed regular stars; (c) and (d) two 4-leafed regular stars; (e) the half-fold ΔOA_1A_2 used in the proof of Corollary 2.

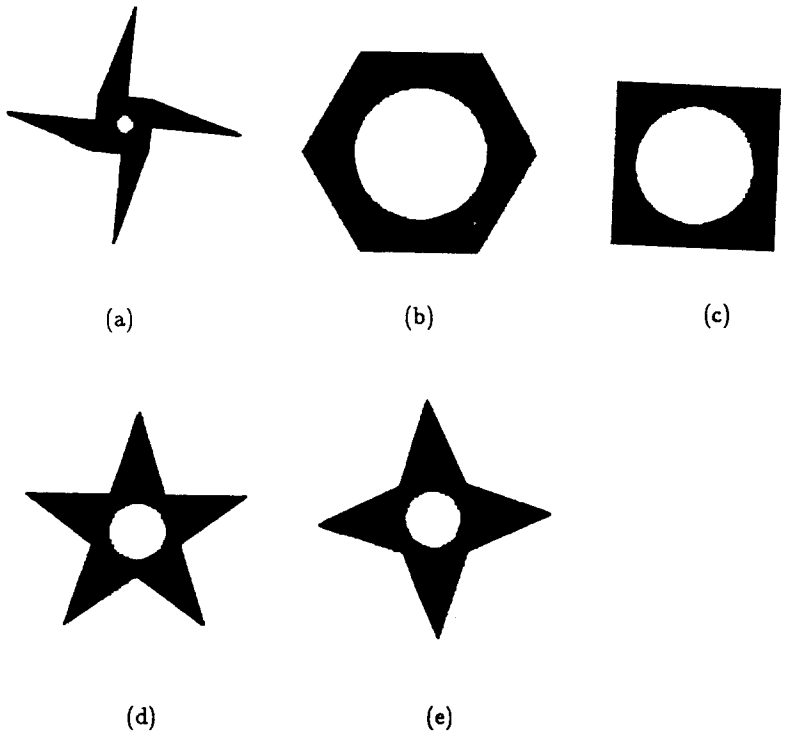

Fig. 6. Examples of shapes satisfying $l_1 = n$ but not radially full. These shapes are identical to the shapes sketched in Fig. 2(b), 3(a), 3(b), 4(a) and 4(c), except that they have holes which are circular disks centered at the centroids of the shapes.

Let $\{p_i\}_{i=1}^{I}$ be the set of all positive factors of l_1 with

$$l_1 = p_1 > p_2 > \cdots > p_I = 1, \tag{7}$$

then $n \in \{p_i\}_{i=1}^{I-1}$. Consequently, the definition of n-RSS given at the beginning of the last section implies that n is the greatest p_i in $\{p_i\}_{i=1}^{I-1}$ satisfying the requirement that the shape S be identical to itself if the shape is rotated through an angle of $2\pi/p_i$. We may therefore try to rotate the shape through an angle of $2\pi/p_1$ and check whether the rotated shape matches the original shape. If it does not, we use the second choice, $2\pi/p_2$, and repeat the rotation-matching procedure until a match is obtained. The value of n is the first p_i that yields an identical match. In summary, n can be detected based on a trial-and-error system using a finite sequence of rotation-matching tests. An algorithm that includes the rotation-matching tests can be found in Reference (1). In the following sections, we derive some conditions in which the rotation -matching tests are no longer needed.

3. SUFFICIENT CONDITIONS TO GUARANTEE THAT $x^{(n)} + iy^{(n)} \neq 0$

In this section we derive conditions to guarantee that the $x^{(n)} + iy^{(n)}$ defined in equation (2) becomes non-zero if the given shape has n folds. When such conditions are satisfied, there is no need to do any rotation-matching test to get the value n, because l_1, which is defined above to be the smallest positive integer l making $x^{(l)} + iy^{(l)} \neq 0$, is just the value n we want. (That $x^{(n)} + iy^{(n)} \neq 0$ can cause $l_1 = n$, may be proven as follows: Theorem 1 implies that all of the numbers l making $x^{(l)} + iy^{(l)} \neq 0$ must belong to the set $\{n, 2n, 3n, \cdots\}$. Hence, $l_1 \geqslant n$. On the other hand, if $x^{(n)} + iy^{(n)} \neq 0$, then n is one of the numbers l making $x^{(l)} + iy^{(l)} \neq 0$, which, by the definition of l_1, means that $n \geqslant l_1$. Together with the inequality $l_1 \geqslant n$, we have $l_1 = n$.)

Lemma 1 below will be used later to prove Theorems 2 and 3. As stated earlier in Section 1, the proofs are all collected in the appendix to make the paper easier to read.

Lemma 1.
Let

$$E = \{(r, \theta) \in S, 0 \leqslant \theta < 2\pi/n\} \tag{8}$$

be a fold of a radially full n-RSS S. If $r_{\max}(\theta)$ of S is monotone in θ when θ is in the interval $[0, 2\pi/n)$, then

$$\int\int_{\{(r,\theta)\in E\}} r^2 \sin n\theta \neq 0. \tag{9}$$

Theorem 2.
If an n-RSS S is

(i) radially full, and
(ii) for some angle β, the boundary points $(r_{\max}(\theta), \theta)$ of S has the property that the function $r_{\max}(\theta)$ is mono-

tone in θ when θ is in the interval $[\beta, \beta + 2\pi/n)$, then $x^{(n)} + iy^{(n)} \neq 0$.

Note that the requirement (ii) above means that there exists a fold in which the polar radii function $r_{\max}(\theta)$ is monotone. (A fold is defined to be the portion of S bounded by any two rays that span an angle of $2\pi/n$.) Here, $\{(r,\theta) \in S | \beta \leqslant \theta < \beta + 2\pi/n\}$ is the fold under discussion. Also note that the monotonicity required above can either be strict monotonicity or weak monotonicity. (Strict increase means that $r_{\max}(\theta_2) > r_{\max}(\theta_1)$ whenever $\theta_2 > \theta_1$; weak increase means that $r_{\max}(\theta_2) \geqslant r_{\max}(\theta_1)$ whenever $\theta_2 > \theta_1$. Strict or weak decrease can be defined likewise.) If the monotonicity is weak, however; it is assumed that $r_{\max}(\theta)$ is not of a single value when θ is in the open interval $(\beta, \beta + 2\pi/n)$. [That is to say, there exist in $(\beta, \beta + 2\pi/n)$ at least two points v and w such that $r_{\max}(v) \neq r_{\max}(w)$.]

As an illustration of the use of Theorem 2, all shapes sketched in Fig. 2 meet the requirements of Theorem 2, and hence, satisfy $l_1 = n$. In Fig. 2(a), the curved boundary in the first quadrant is the curve $\{(r_{\max}(\theta), \theta) | 0 \leqslant \theta < \pi/2\}$ with $r_{\max}(\theta) = \cos\theta$ which meets the monotonicity property of $r_{\max}(\theta)$ stated in Theorem 2. In Fig. 2(b), it has been assumed that $\angle OCA \geqslant \pi/2$ and $\angle OAB \geqslant \pi/2$ where O is the centroid. By the law that the larger angle is opposite to the larger side in every triangle, we claim that $r_{\max}(\theta)$ is decreasing as the boundary point $(r_{\max}(\theta), \theta)$ moves along line segment $\overline{BA}$ from B through A, and then moves along line segment $\overline{AC}$ from A through C. In Fig. 2(c), $r_{\max}(\theta) = 1$ when $0 \leqslant \theta < \pi/4$, and $r_{\max}(\theta) = 0$ when $\pi/4 \leqslant \theta < \pi/2$. The monotone property is therefore in the weak sense.

4. WHEN THE RSS IS ALSO MIRROR SYMMETRIC

If an n-RSS S contains a fold which is mirror symmetric about a ray $\theta = \beta$, then the monotone property of the $r_{\max}(\theta)$ used in Theorem 2 can be modified to be monotone in one half of a fold, instead of being monotone throughout the whole fold. This leads to the theorem below. As in Theorem 2, the monotonicity can be either strict or weak.

Theorem 3.
If an n-RSS S is

(i) radially full,
(ii) for some angle β, the boundary points $(r_{\max}(\theta), \theta)$ of S has the property that the function $r_{\max}(\theta)$ is monotone in θ when θ is in the interval $[\beta, \beta + \pi/n)$, and
(iii) the fold $\{(r,\theta) \in S | \theta \in [\beta - \pi/n, \beta + \pi/n]\}$ itself is mirror symmetric about the ray $\theta = \beta$,

then $x^{(n)} + iy^{(n)} \neq 0$

Notice that the interval in Condition (ii) here is only one half of the interval mentioned in Condition (ii) of Theorem 2. Several direct applications of Theorem 3 are described as corollaries below.

Corollary 1.
For every regular polygon of n sides (see Fig. 3), we have $x^{(n)} + iy^{(n)} \neq 0$.

Definition 3.
Let θ_1, r_1, r_2 represent three constants, and let $r_1 > r_2 > 0$. An n-leafed regular star ($n \geqslant 3$) is a radially full n-RSS with $2n$ corners $\{A_j\}_{j=1}^{2n}$, and whose boundary is the union of $2n$ line segments $\{\overline{A_j A_{j+1}}\}_{j=1}^{2n}$ where $A_1 = A_{2n+1}$, and the polar coordinate of each corner A_j is $(r_1, \theta_1 + (j-1)\pi/n)$ or $(r_2, \theta_1 + (j-1)\pi/n)$, according to whether the value j is odd or even.

[Two 5-leafed regular stars and two 4-leafed regular stars are sketched in Fig. 4(a) through 4(d).]

Corollary 2.
If S is an n-leafed star, then $x^{(n)} + iy^{(n)} \neq 0$.

The n-leafed rose is a kind of shape often encountered in mathematics field [for example, see Reference (10)]. The definition of an n-leafed rose depends on whether n is even or odd. A 4-leafed rose and a 3-leafed rose are sketched in Fig. 5.

Definition 4.
Let n, a, θ_0 be three given constants with n even and $a > 0$. Then an n-leafed rose is an n-RSS, of which the first fold is defined as the area enclosed by the curve $\{(r_{\max}(\theta), \theta) | r_{\max}(\theta) = a\sin\frac{n}{2}(\theta - \theta_0), \theta_0 \leqslant \theta < \theta_0 + 2\pi/n\}$. *The other* $n-1$ folds are defined by a sequence of rotations of this fold through angles of multiples of $2\pi/n$.

Definition 5.
Let n, a, θ_0 be three given constants with n odd and $a > 0$. Then an n-leafed rose is an n-RSS, of which the first fold is defined as the area enclosed by the curve $\{(r_{\max}(\theta), \theta) | \theta_0 \leqslant \theta < \theta_0 + 2\pi/n\}$, and where

$$r_{\max}(\theta) = \begin{cases} a\sin n(\theta - \theta_0), & \text{if } \theta_0 \leqslant \theta < \theta_0 + \pi/n; \\ 0, & \text{if } \theta_0 + \pi/n \leqslant \theta < \theta_0 + 2\pi/n. \end{cases}$$

The other $n-1$ folds are defined by a rotation of this fold through angles of multiples of $2\pi/n$.

Because $\sin(t)$ is an increasing function of t when $t \in (0, \pi/2)$, we can obtain Corollary 3 below. The details of the proof are omitted for brevity's sake.

Corollary 3.
$x^{(n)} + iy^{(n)} \neq 0$ for every n-leafed rose.

In the theorems and corollaries above, we have assumed that the shape is radially full. This requirement can be modified slightly, however, if the radially full shape is punched such that the new shape contains a hole that is a circular disk centered at the centroid of the original shape. An example of this is a bolt nut, which is the region whose exterior boundary is a regular polygon, and whose interior boundary is a circular disk [see Fig. 6(b) and (c) for illustrations]. The proof for this modified version is identical to the original proofs of Theorems 2 and 3 and is hence omitted.

Also note, that, based on the proofs given in the appendix [see (A4) and (A9)], the monotone condition

(ii) in both Theorems 2 and 3 can be weaken somewhat. More precisely, the (ii) in Theorem 2 can be replaced by either (iia) or (iib); whereas the (ii) in Theorem 3 can be replaced by either (iic) or (iid). They are stated below:

(iia) For some angle β, the boundary points $(r_{\max}(\theta), \theta)$ of S has the property that $r_{\max}(\theta) \geqslant r_{\max}(\theta + \pi/n)$ for all θ in the interval $[\beta, \beta + \pi/n)$, and "$>$" holds on at least a subinterval of $[\beta, \beta + \pi/n)$.

(iib) (Replace the "$\geqslant$" and "$>$" of (iia) by "$\leqslant$" and "$<$", respectively.)

(iic) For some angle β, the boundary points $(r_{\max}(\theta), \theta)$ of S has the property that $r_{\max}(\beta + \pi/2n - \theta) \geqslant r_{\max}(\beta + \pi/2n + \theta)$ for all θ in the interval $(0, \pi/2n)$, and "$>$" holds on at least a subinterval of $(0, \pi/2n)$.

(iid) (Replace the "$\geqslant$" and "$>$" of (iic) by "$\leqslant$" and "$<$", respectively.)

Note that the wordy conditions (iia)–(iid) are easier to use, whereas the compact condition (ii) is easier to state and memorize (because people are more familiar with the tacit meaning of the conventional term "monotone").

5. EXPERIMENTATION

In practice, the $x^{(l)} + iy^{(l)}$ defined in equation (2) is evaluated using

$$\sum_{k=1}^{K} |x_k + iy_k| \left(\frac{x_k + iy_k}{|x_k + iy_k|} \right)^l \tag{10}$$

where K is the number of sampled points contained in the shape. Because sampling and rounding errors may both exist, the l_1 mentioned in sections above should be detected using a more practical rule. In other words, instead of identifying l_1 as the smallest positive integer that satisfies $x^{(l_1)} + iy^{(l_1)} \neq 0$, we identify l_1 as the smallest positive integer making

$$\frac{|x^{(l_1)} + iy^{(l_1)}|}{K} \gg \text{MAX}\left\{ \frac{|x^{(l_1-1)} + iy^{(l_1-1)}|}{K}, \frac{|x^{(l_1+1)} + iy^{(l_1+1)}|}{K} \right\}. \tag{11}$$

The reason why we divide the values of $x^{(l)} + iy^{(l)}$ by K is stated in Reference (1).

The author has performed several experiments using some shapes stated in Theorem 2. The author has also performed a sequence of experiments to detect the fold number n, with n ranges from 3 through 10, for roses, regular polygons, regular stars, and bolt nuts. The experimental results show that the obtained value of l_1 is the expected value of n. For example, when a 4-side regular polygon formed of $K = 45369$ sampled points is used in the experiment, the values of $\{|x^{(l)} + iy^{(l)}|/45369\}_{l=1}^{5}$ obtained by a SUN-ELC workstation are all less than 10^{-15}, the only exception being when $l = 4$, which yields a much bigger value, namely, $|x^{(4)} + iy^{(4)}|/\,45369 = 17.49089901$. The polygon is therefore concluded to be four sided without doing any rotation or matching process. Some other experimental results are listed in Fig. 7. All shapes used

l	The computed values $\lvert x^{(l)} + iy^{(l)}\rvert/K$			
2	0.00000000	0.04412934	0.03696307	0.00000000
3	0.00000000	0.01115491	0.07068337	0.00000000
4	(37.27632301)	0.00650382	0.18736826	(36.2230002)
5	0.00000000	0.00656115	(46.4089416)	0.00000000
6		(8.0679111)	0.25721887	
7		0.00336123		
SHAPE	*Fig* 2(*b*) (a 4-fold windmill) (K = 13181 points)	*Fig.* 3(*a*) (a 6-side polygon) (K = 58394 points)	*Fig.* 4(*b*) (a 5-leafed star) (K = 13545 points)	*Fig.* 4(*c*) (a 4-leafed star) (K = 25307 points)

l	The computed values $\lvert x^{(l)} + iy^{(l)}\rvert/K$			
2	0.00792683	0.42327463	0.00000000	0.62949276
3	0.08226388	(48.980283)	0.00000000	0.15918286
4	(33.59730941)	0.52830236	(39.258304)	0.10564380
5	0.104877459		0.00000000	0.09614510
6				(11.50829694)
7				0.05603174
SHAPE	*Fig* 5(*a*) (a 4-leafed rose) (K = 15707 points)	*Fig.* 5(*b*) (a 3-leafed rose) (K = 8040 points)	*Fig.* 6(*a*) (a 4-RSS) (K = 12516 points)	*Fig.* 6(*d*) (a 6-side bolt nut) (K = 40937 points)

Fig. 7. The computed values of $\{|x^{(l)} + iy^{(l)}|/K\}_{l=1}^{l_1+1}$ for some shapes sketched in the previous figures. As usual, K denotes the number of the sampled points in the shape. For each shape, the reader can see that the l corresponding to the first "pulse" value (the enclosed entry) really gives the expected fold number of the shape.

in the experiment were computer-generated, i.e., they were generated by simulation. Each shape, together with the (white) background, formed an $m \times m$ black-and-white image with m ranging from 150 to 300. Among the m^2 sampled points, only K points belonged to the shape (and the remaining m^2-K points belonged to the background). Therefore, $K \leqslant m^2$ and $22500 \leqslant m^2 \leqslant 90000$. The actual values of K were indicated in Fig. 7.

6. SUMMARY AND CONCLUDING DISCUSSION

It is proved in this paper that the fold number n of certain kinds of shapes, including roses, bolt nuts and regular polygons, can be identified as the smallest natural number l making $x^{(l)} + iy^{(l)}$ non zero. The matching process, which is used in many reported methods, is not used at all in the proposed computing scheme. Hence, detecting fold numbers for these kinds of shapes is much easier. Note that the proposed algorithm stops at the iteration corresponding to fold number n. [Or, if sampling error is considered, stops at the $(n+1)$-th iteration, as is shown in Fig. 7.] Some other reported methods that try to avoid matching process have to do many iterations after the n-th iteration. Usually, $3n$ or more iterations are used in these methods [see the last paragraph of Section 5 in Reference (1)]. Therefore, these methods are not as fast as the method proposed here.

In Reference (1), Lin *et al.* proved that the shape orientation can be obtained without further computation whenever the value n of the fold number is obtained using their computing scheme (in their words, "the orientation of the given rotationally symmetric shape is a by-product of the fold number detection method"). Since the computing scheme presented here is just a simplified version of their scheme (we just bypass the non-necessary rotation-matching test used in Reference (1) when the shapes are regular polygons, bolt nuts, etc.), the shape orientation can also be obtained immediately without further computation. In fact, once the value n is obtained, we just define the shape orientation to be the half-line ejected from the centroid and with the directional angle $1/n$ angle $(x^{(n)} + iy^{(n)})$. Therefore, shape orientation, together with fold number n, can both be detected quickly for regular polygons, bolt nuts, roses, etc.

Acknowledgement—This work was supported by the National Science Council, Republic of China, under contract number NSC80-0408-E-009-26. The author also thanks the referee for the clear revision guideline.

APPENDIX

Proof of Lemma 1

Without the loss of generality, we prove the case that $r_{max}(\theta)$ is decreasing. Decompose E into two disjoint half-folds $E = E' \bigcup E''$ where $E' = \{(r,\theta) \in S | 0 \leqslant \theta < \pi/n\}$ and $E'' = \{(r, \theta) \in S | \pi/n \leqslant \theta < 2\pi/n\}$, respectively. Because S is radially full, the term in the right hand side of equation (9) can be expressed as

$$\int_0^{2\pi/n}\int_0^{r_{max}(\theta)} r^2 \sin n\theta \, dr d\theta = \int_0^{2\pi/n} \tfrac{1}{3} r_{max}^3(\theta) \sin n\theta \, d\theta$$
$$= \int_0^{\pi/n} \tfrac{1}{3} r_{max}^3(\theta) \sin n\theta \, d\theta + \int_{\pi/n}^{2\pi/n} \tfrac{1}{3} r_{max}^3(\theta) \sin n\theta \, d\theta. \tag{A1}$$

Notice that

$$\int_{\pi/n}^{2\pi/n} \tfrac{1}{3} r_{max}^3(\theta) \sin n\theta \, d\theta = -\int_{\pi/n}^{2\pi/n} \tfrac{1}{3} r_{max}^3(\theta) \sin n(\theta - \pi/n) d\theta$$
$$= -\int_0^{\pi/n} \tfrac{1}{3} r_{max}^3(\hat{\theta} + \pi/n) \sin n\hat{\theta} \, d\hat{\theta} \tag{A2}$$

where (A2) is derived by introducing a new variable $\hat{\theta} = \theta - \pi/n$. On the other hand, $\int_0^{\pi/n} \frac{1}{3} r_{max}^3(\hat{\theta} + \pi/n) \sin\eta\hat{\theta} d\hat{\theta}$ and $\int_0^{\pi/n} \frac{1}{3} r_{max}^3(\theta + \pi/n) \sin n\theta d\theta$ are the same amount expressed in distinct notations; therefore, equation (A2) implies that

$$\int_{\pi/n}^{2\pi/n} \tfrac{1}{3} r_{max}^3(\theta) \sin n\theta \, d\theta = -\int_0^{\pi/n} \tfrac{1}{3} r_{max}^3(\theta + \pi/n) \sin n\theta d\theta. \tag{A3}$$

As a result, equation (A2) can be reduced to

$$\int_0^{2\pi/n}\int_0^{r_{max}(\theta)} r^2 \sin n\theta \, dr d\theta$$
$$= \int_0^{\pi/n} \tfrac{1}{3} r_{max}^3(\theta) \sin n\theta \, d\theta - \int_0^{\pi/n} \tfrac{1}{3} r_{max}^3(\theta + \pi/n) \sin n\theta d\theta$$
$$= \int_0^{\pi/n} \tfrac{1}{3} (r_{max}^3(\theta) - r_{max}^3(\theta + \pi/n)) \sin n\theta d\theta$$
$$> 0. \tag{A4}$$

In the derivation of equation (A4), we have used the fact that $r_{max}(\theta) > r_{max}(\theta + \pi/n)$, for all $\theta \in [0, \pi/n)$, if the decrease property of r_{max} is strict. □

Remark. (Weak monotonicity case).

If the decrease property of r_{max} is in the weak sense, however, the proof of Inequality (A4) is a little longer. In this case, we only have to prove that $r_{max}(\theta) > r_{max}(\theta + \pi/n)$ on a (small) subinterval of $(0, \pi/n)$. Because we had stated in the text that there exists at least a pair v, w in the interval $(0, 2\pi/n)$ such that $r_{max}(v) \neq r_{max}(w)$, we may then assume that $0 < v < w < 2\pi/n$ and $r_{max}(v) > r_{max}(w)$. There are three possible cases for the locations of u and v, namely, $v < w \leqslant \pi/n$; $\pi/n \leqslant v < w$; $v < \pi/n < w$. If $v < w \leqslant \pi/n$, then

$$r_{max}(\theta) \geqslant r_{max}(v) > r_{max}(w) \geqslant r_{max}\left(\frac{\pi}{n}\right) \geqslant r_{max}\left(\theta + \frac{\pi}{n}\right)$$

for all $\theta \in (0, v)$.

Equation (A4) is therefore obtained again. If $\pi/n \leqslant v < w$, a similar argument will work. If $v < \pi/n < w$, we may still proceed as follows. Use $r_{max}(v) \geqslant r_{max}(\pi/n) \geqslant r_{max}(w)$ and $r_{max}(v) > r_{max}(w)$ to conclude that either $r_{max}(v) > r_{max}(\pi/n)$ or $r_{max}(\pi/n) > r_{max}(w)$. If $r_{max}(v) > r_{max}(\pi/n)$, then $r_{max}(\theta) \geqslant r_{max}(v) > r_{max}(\pi/n) \geqslant r_{max}(\theta + \pi/n)$ for all $\theta \in (0, v)$. If $r_{max}(\pi/n) > r_{max}(w)$, an analogous argument will work.

□

Proof of Theorem 2.

Whether $x^{(l)} + iy^{(l)}$ is zero or not has nothing to do with the phases of the given shape S. We therefore only have to prove the theorem for the case $\beta = 0$. Substituting $l = n$ into Equa-

tion (4), we have

$$x^{(n)}+iy^{(n)}=\int_0^{2\pi}\int_0^{r_{\max}(\theta)} r^2 e^{in\theta}\,dr\,d\theta=\int_0^{2\pi}\tfrac{1}{3}r_{\max}^3(\theta)e^{in\theta}\,d\theta$$

$$=\int_0^{2\pi/n}+\int_{2\pi/n}^{4\pi/n}+\int_{4\pi/n}^{6\pi/n}+\cdots+\int_{2(n-1)\pi/n}^{2\pi}[\tfrac{1}{3}r_{\max}^3(\theta)e^{in\theta}]\,d\theta$$

$$=\int_0^{2\pi/n}\tfrac{1}{3}r_{\max}^3(\theta)e^{in\theta}\,d\theta+\int_0^{2\pi/n}\tfrac{1}{3}r_{\max}^3(\theta+2\pi/n)e^{in(\theta+2\pi/n)}\,d\theta$$

$$+\int_0^{2\pi/n}\tfrac{1}{3}r_{\max}^3(\theta+4\pi/n)e^{in(\theta+4\pi/n)}\,d\theta+\cdots$$

$$=n\int_0^{2\pi/n}\tfrac{1}{3}r_{\max}^3(\theta)e^{in\theta}\,d\theta \tag{A5}$$

$$=n\left(\int_0^{2\pi/n}\tfrac{1}{3}r_{\max}^3(\theta)\cos n\theta\,d\theta+i\int_0^{2\pi/n}\tfrac{1}{3}r_{\max}^3(\theta)\sin n\theta\,d\theta\right). \tag{A6}$$

The derivation of equation (A5) uses the fact that both $r_{\max}(\theta)$ and $e^{in\theta}$ are cyclic with period $2\pi/n$. Note that equation (A6) then implies that it is sufficient to show that $\int_0^{2\pi/n}\frac{1}{3}r_{\max}^3(\theta)\sin n\theta\,d\theta\neq 0$; or equivalently, to show that $\int_0^{2\pi/n}\int_0^{r_{\max}(\theta)}r^2\sin n\theta\,dr\,d\theta\neq 0$. However, this is exactly the statement claimed by Lemma 1. □

Proof of Theorem 3.
We only have to prove the theorem for the case $\beta=0$. Equation (A6) then implies that we only have to show that $\int_0^{2\pi/n}r_{\max}^3(\theta)\cos n\theta\,d\theta$ is non-zero. The remaining proof is divided into two parts: Parts I and II.

Part I. (Showing that $\int_0^{2\pi/n}r_{\max}^3(\theta)\cos n\theta\,d\theta=2\int_0^{\pi/n}r_{\max}^3(\theta)\cos n\theta\,d\theta$.)
First note that

$$\int_0^{2\pi/n}r_{\max}^3(\theta)\cos n\theta\,d\theta=\int_0^{\pi/n}+\int_{\pi/n}^{2\pi/n}=\int_0^{\pi/n}+\int_{-\pi/n}^{0} \tag{A7}$$

Since $r_{\max}(\theta)=r_{\max}(-\theta)$, we have $\int_{-\pi/n}^{0}r_{\max}^3(\theta)\cos n\theta\,d\theta=\int_{-\pi/n}^{0}r_{\max}^3(-\theta)\cos n(-\theta)\,d\theta=\int_{\pi/n}^{0}[r_{\max}^3(u)\cos nu][-du]=\int_0^{\pi/n}r_{\max}^3(u)\cos nu\,du$ where $u=-\theta$. Equation (18) can thus be written as $\int_0^{2\pi/n}r_{\max}^3(\theta)\cos n\theta\,d\theta=\int_0^{\pi/n}r_{\max}^3(\theta)\cos n\theta\,d\theta+\int_0^{\pi/n}r_{\max}^3(u)\cos nu\,du=2\int_0^{\pi/n}r_{\max}^3(\theta)\cos n\theta\,d\theta$.

Part II. (Showing that $\int_0^{\pi/n}r_{\max}^3(\theta)\cos n\theta\,d\theta\neq 0$.)
We first introduce a new variable $\lambda=\pi/2n=\theta$ to derive

$$\int_0^{\pi/2n}r_{\max}^3(\theta)\cos n\theta\,d\theta=\int_0^{\pi/2n}(r_{\max}^3(\theta))[\sin n(\pi/2n-\theta)]\,d\theta$$

$$=\int_{\pi/2n}^{0}r_{\max}^3(\pi/2n-\lambda)[\sin n(\lambda)](-d\lambda)$$

$$=\int_0^{\pi/2n}r_{\max}^3(\pi/2n-\lambda)[\sin n\lambda]\,d\lambda.$$

We then introduce another variable $\hat{\theta}=\theta-\pi/2n$ to derive

$$\int_{\pi/2n}^{\pi/n}r_{\max}^3(\theta)\cos n\theta\,d\theta=\int_{\pi/2n}^{\pi/n}(r_{\max}^3(\theta))[-\sin n(\theta-\pi/2n)]\,d\theta$$

$$=-\int_0^{\pi/2n}r_{\max}^3(\pi/2n+\hat{\theta})\sin n\hat{\theta}\,d\hat{\theta}. \tag{A8}$$

Therefore,

$$\int_0^{\pi/n}r_{\max}^3(\theta)\cos n\theta\,d\theta$$

$$=\int_0^{\pi/2n}r_{\max}^3(\theta)\cos n\theta\,d\theta+\int_{\pi/2n}^{\pi/n}r_{\max}^3(\theta)\cos n\theta\,d\theta$$

$$=\int_0^{\pi/2n}r_{\max}^3(\pi/2n-\lambda)\sin n\lambda\,d\lambda-\int_0^{\pi/2n}r_{\max}^3(\pi/2n+\hat{\theta})\sin n\hat{\theta}\,d\hat{\theta}$$

$$=\int_0^{\pi/2n}(r_{\max}^3(\pi/2n-0)-r_{\max}^3(\pi/2n+0))\sin n\theta\,d\theta$$

$$>0 \tag{A9}$$

because $\sin n\theta$ is positive and $r_{\max}^3(\pi/2n-0)>r_{\max}^3(\pi/2n+0)$ when $0<\theta<\pi/2n$. Here, we had assumed that $r_{\max}(\theta)$ is strictly decreasing. However, equation (A9) is still greater than zero if $r_{\max}(\theta)$ is weakly decreasing and non-constant on the interval $(0,\pi/2n)$. The proof is the same as those given in the proof of Lemma 1, and is hence omitted. □

Proof of Corollary 1.
Let O be the centroid of the polygon S. Let C be the middle point of a polygon edge $\overline{AB}$. Condition (iii) is guaranteed because the fold ΔAOB is mirror symmetric about the line segment $\overline{OC}$. The monotone property (ii) is obvious as the boundary point $(r_{\max}(\theta),\theta)$ moves along the line segment $\overline{AC}$ from corner A to C. □

Proof of Corollary 2[see Fig. 4(e)].
First, note that every regular star is both radially full and mirror-symmetric. Then look at the half-fold ΔOA_1A_2 with $O=(0,0)$, $A_1=(r_1,\theta_1)=(r_1,O)$, and $A_2=(r_2,\theta_1+\pi/n)=(r_2,\pi/n)$. Let $H\in\overline{A_1,A_2}$ be such that $\overline{OA_2}$ bisects the angle $\angle A_1OA_2$. Since $r_1>r_2$, we have $\angle OA_2A_1>\angle OA_1A_2$. As a result, $\angle OHA_1>\angle OHA_2$ can be derived using $\angle OA_2A_1+\angle A_2OH>\angle OA_1A_2+\angle A_1OH$. Therefore, $r_{\max}^3(\pi/2n-0)>r_{\max}^3(\pi/2n+0)$ when $0<\theta<\pi/2n$. Equation (A9) is therefore strictly positive. The proof of Theorem 3 [from the very beginning of that proof to equation (A9)] can then be used. □

REFERENCES

1. J. C. Lin, W. H. Tsai and J. A. Chen, Detecting number of folds by a simple mathematical property, *Pattern Recognition-Lett.* **15**, 1081–1088 (1994).
2. J. J. Leou and W. H. Tsai, Automatic rotational symmetry determination for shape analysis, *Pattern Recognition* **20**, 571–582 (1987).
3. S. L. Chou, J. C. Lin and W. H. Tsai, Fold-principal axis—a new tool for defining the orientations of rotationally symmetric shapes, *Pattern Recognition Lett.* **12**, 109–115 (1991).
4. S. K. Parui and D. D. Majumder, Symmetry analysis by computer, *Pattern Recognition* **16**, 63–67 (1993).
5. P. T. Highnam, Optimal algorithm for finding the symmetries of a planar point set, *Inf. Process. Lett.* **22**, 219–222 (1986).
6. M. J. Atallah, On symmetry detection, *IEEE Trans. Comput.* **34**, 663–666 (1985).
7. J. C. Lin, S. L. Chou and W. H. Tsai, Detection of rotationally symmetric shape orientations by fold-invariant shape-specific points, *Pattern Recognition* **25**, 473–482 (1992).
8. G. Marola, On the detection of the axes of symmetry of symmetric and almost symmetric planar images, *IEEE Trans.* **PAMI-11**, 104–108 (1989).
9. F. P. Preparata and M. I. Shamos, *Computational Geometry*, Springer-Verlag, New York (1985).
10. R. E. Larson and R. P. Hostetler, *Calculus with Analytic Geometry*, 2nd ed., Heath and Company (1982).

About the Author—JA-CHEN LIN was born in 1955 in Taiwan, Republic of China. He received his B.S. degree in computer science in 1977 and M.S. degree in applied mathematics in 1979, both from National Chiao Tung University, Taiwan. In 1988 he received his Ph.D. degree in mathematics from Purdue University, U.S.A.

In 1981–1982 he was an instructor at National Chiao Tung University. From 1984 to 1988, he was a graduate instructor at Purdue University. He joined the Department of Computer and Inforamtion Science at National Chiao Tung University in August 1988, and is currently an Associate Professor there. His recent research interests include pattern recognition, image processing, and parallel computing. Dr Lin is a member of the Phi-Tau-Phi Scholastic Honor Society.